DE GRUYTER OPEN

Acta Geophysica
vol. 64, no. 6, Dec. 2016, pp. 2794-2809
DOI: 10.1515/acgeo-2016-0114

Ranking of Sudden Ionospheric Disturbances by Means of the Duration of Vlf Perturbed Signal in Agreement with Satellite X-Ray Flux Classification

Ahmed AMMAR and Hassen GHALILA

Laboratoire de Spectroscopie Atomique, Moléculaire et Applications (LSAMA), Faculty of Science, University of Tunis El Manar, Tunis, Tunisia;
e-mails: ammarahmed.ph@gmail.com (corresponding author), ghalila.sevestre@wanadoo.tn

Abstract

Ionosphere undergoes permanently solar flares that quickly change its properties inducing sometime unwanted effects. These changes, or events, are known as Sudden Ionospheric Disturbances (SIDs) and the knowledge of their magnitude may be of great interest to anticipate probable damages. Currently, there does not exist any classification of these ionospheric changes based on their amplitude due to the wide variability of its responses. The only way to surmise their importance is to study them indirectly, throughout the classification of the X-ray flux intensity recorded by satellites. An attempt of classification based on their duration was proposed by the American Association of Variable Star Observers (AAVSO) but it is not very accurate because SID's duration is measured directly from the raw signal of the Very Low Frequency (VLF) signal and/or the Low Frequency (LF) signal. The aim of this work is to investigate, through a set of simple mathematical techniques applied to VLF/LF signals recorded by ground based receivers, the best method to estimate SIDs durations and then propose a new classification based on these durations.

Key words: VLF/LF, SIDs' classification, statistical ACP method, EMD method.

1. INTRODUCTION

The study of the Sun and its effects on the ionosphere is one of the many themes studied by the United Nations International Space Weather Initiative (ISWI). Among the many devices used for this topic, the Sudden Ionospheric Disturbance (SID) monitors (Scherrer *et al.* 2008) are a ground based VLF (Very Low Frequency) receivers dedicated to study Sudden Ionospheric Disturbances (SIDs) (Dellinger 1937). Those SIDs occur in association with solar flares and may have a very strong and relatively long-lasting effect on the ionosphere (Thomson and Clilverd 2001, Grubor *et al.* 2008). Indeed, the more intense the solar flares, the more important are their effects on the Earth. Therefore, the knowledge of the magnitude of a solar flare is crucial to prevent unwanted problems. This is the reason why these flares are closely monitored and classified with respect to X-ray fluxes intensity recorded by GOES satellites since the 1970s by the National Oceanic and Atmospheric Administration (NOAA) Space Weather Scales (SWPC/NOAA 2015).

Strong solar storms have been known as the most devastating solar effects that can cause satellites' entire failure or lead to communications blackout. We can mention as an example the "Halloween Storm" of October-November 2003, which is the strongest solar activity, the near-Earth space environment ever experienced in recent history (Rosen and Johnson 2004). Furthermore, during that period one of the solar flares had saturated the GOES's X-ray sensors, which made the estimation of its intensity difficult and consequently it was not classified. To overcome this problem, a study of the amplitude and phase of SID recorded by a ground VLF radio receiver (Thomson *et al.* 2005) succeed to give a reasonable estimation to the real intensity of this great solar flare. This example reveals the need to find another reliable method to classify solar events as an alternative to the NOAA one.

Due to the many parameters that govern the behaviour of the ionosphere (*e.g.*, solar cycle activity, seasonal period, day-night variation, path of the VLF from the transmitter to the receiver, chemical processes, *etc*.) (Mitra 1975, Dahlgren *et al.* 2011, Correia *et al.* 2011), the lasting effect of the flares is highly variable. Until the current day, there is only one rough technique used to classify the SIDs, which is based on their duration (AAVSO 2015). In other words, instead of asking the classical question: How strong is the effect of solar flare on the ionosphere? We ask the question: How much time does the effect of solar flare remain on the ionosphere? We propose, in the present work, new approaches to improve this method. To do this, we compare SIDs events observed from a ground VLF/LF recording (SID monitor) with solar flares observed from out space by NOAA's GOES satellite

sensors. A special care is given for the treatment of the VLF recording and the assessment of the event's duration. In Section 1 we present the typical VLF signals and the way to identify a SID. In the Section 2 we present the different methods used to measure the event's duration on VLF recording obtained during June 2012. The last Section is dedicated to the discussion and the description of the criteria chosen for the classification.

2. VLF RECORDING AND SIDs

SID monitors daily VLF by recording, every five seconds, VLF radio waves propagating in the earth-ionosphere waveguide. It is worth noting that the SID monitor records only the amplitude of the VLF/LF signal (no phase information is recorded). In the present work we have used data recorded by the SID monitor installed at the Faculty of Sciences of Tunis (FST) (36.833° N, 10.133° E), which has been tuned to the radio-VLF transmitter NAA operating at 24.00 kHz in Maine, USA (44.633° N, 67.267° W). Figure 1 shows the Great Circle Path (GCP) between the VLF transmitter station (Maine) and the VLF receiver station (Tunis) which is ~ 6326 km.

Figure 2 illustrates the diurnal and seasonal changes of amplitude of VLF signals; Fig. 2a corresponds to winter condition and Fig. 2b corresponds to summer condition. We can see from both figures, 2a and 2b, that the most stable part of the data is the part (C), when the GCP of the VLF wave is totally in the Earth's day side. This part of the signal will be referred to as "quiet diurnal level" for the remaining of the document.

We limit all record's analyzes to the diurnal zone, when the majority of the GCP is in the Earth's day-side. The detection of SID events is to track down

Fig. 1. Great Circle Path (GCP) between the NAA transmitter (24 kHz) and receiver at Tunis over a distance of ~6326 km.

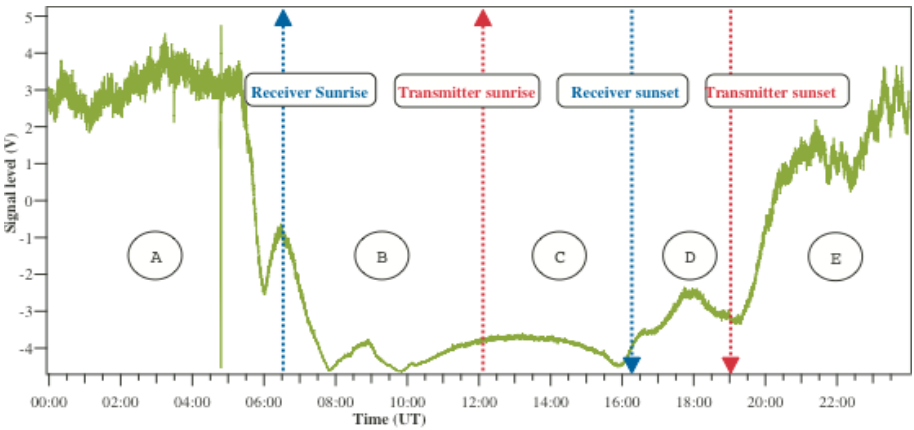

(a) Tunis/NAA VLF signal recorded on 1 January 2012

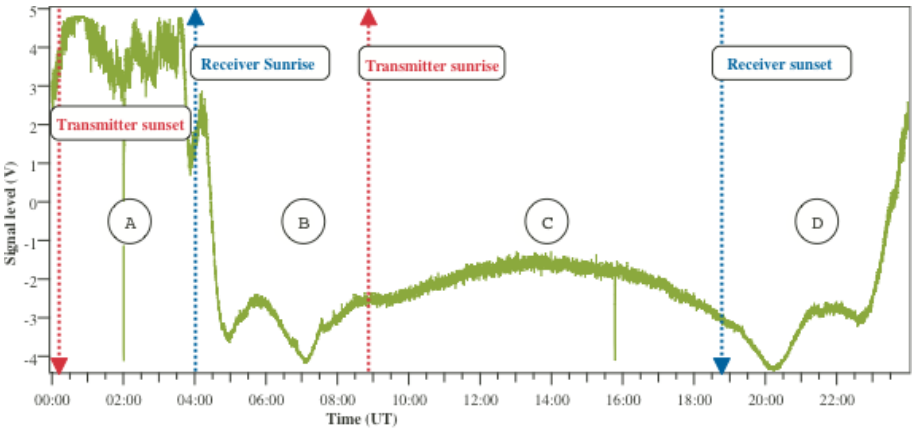

(b) Tunis/NAA VLF signal recorded on 20 June 2012

Fig. 2. Variation of the data level of NAA (USA)-LSAMA (Tunisia) for a day without solar flares. We can see that the signal is divided to four parts depending on the elevation of the sun on both receiver and transmitter locations. Parts (A) and (E) are when the GCP of VLF wave is totally in the Earth's night-side, parts (B) and (D) are when the GCP is partially in the Earth's day-side, and part (C) is when GCP is totally in the Earth's day-side.

any disturbances from the quiet diurnal level. Then we systematically compare VLF recording with GOES X-ray Flux to make sure that these disturbances are induced by solar flares.

The shape of SID events depends on some factors, such as the distance between the transmitting and receiving stations, as well as the temporal vari-

ation of ionospheric parameters. They could have an increase in amplitude, some have an amplitude decrease, some have complex shapes in time (*e.g.*, a decrease below the unperturbed values that followed some of the strong increases in VLF signal) and in some cases the amplitude can be saturated. This variation in SID's shape could be investigated by comparing it with signals produced by a waveguide propagation model (Dahlgren *et al.* 2011). Analyses presented here are limited to SID events detected on signal coming from NAA transmitter and received at Tunis. All the SIDs have similar shapes with a positive increase in amplitude without any saturation. The module can be applied directly to SIDs with negative variation as well. As an example, Fig. 3b shows the signal of the 9 June 2012, involving three events close to 10:29, 11:30, and 16:48 UT. Comparing this signal to the X-ray Flux recorded by the GOES satellite (Fig. 3a) for the same day we can note the almost perfect synchronization with measured solar flares.

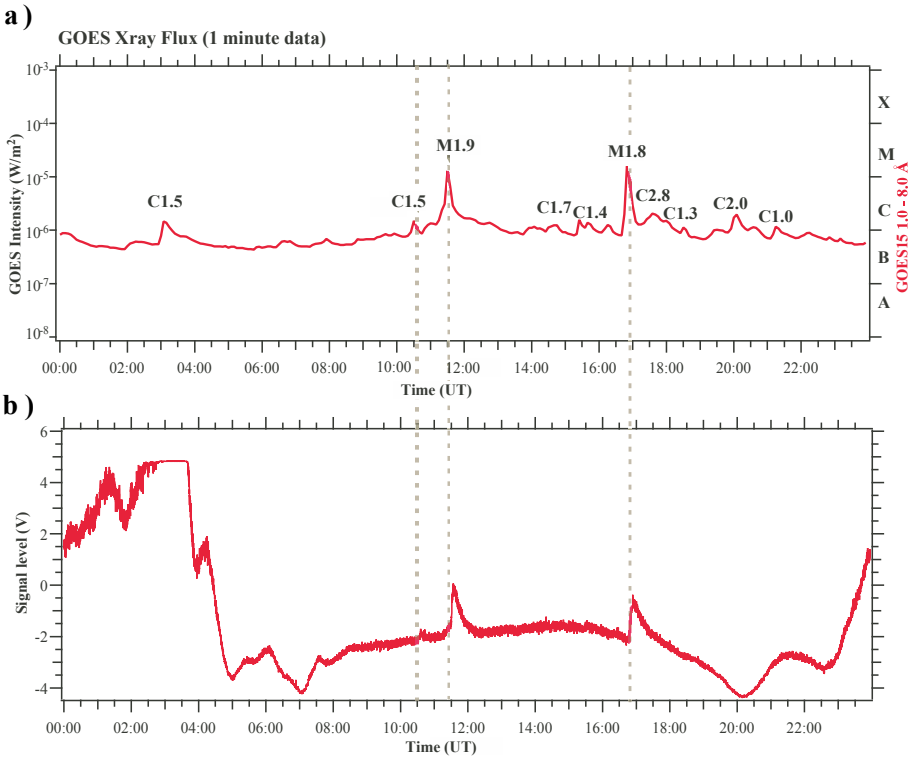

Fig. 3. Identification of the SID events with the GOES Flux. Dashed lines show how the identification is done. (a) X-ray Flux from the Sun observed from GOES satellite during 9 June 2012, and (b) Ground VLF amplitude observed from Tunis during 9 June 2012.

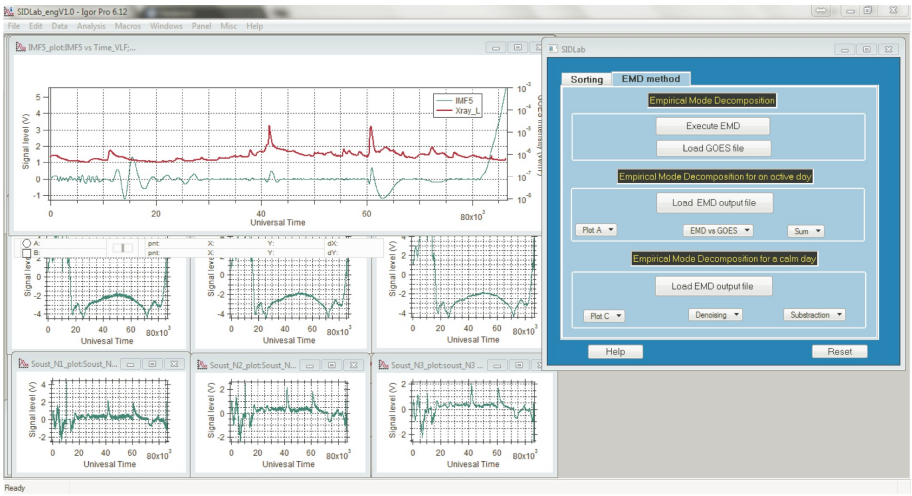

Fig. 4. Screen capture of SIDLab application developed under Igor Pro software (https://www.wavemetrics.com/).

This ascertainment allows us to conclude that these three events correspond to SIDs events. To make all these processes faster and also the methods applied in this work more efficient, we gathered all in one application called "SIDLab", whose interface is shown in Fig. 4.

3. SIGNAL PROCESSING OF JUNE 2012 VLF RECORDING

In this section, we describe and test several methods in order to estimate the length of SIDs. These methods are applied to data recorded during the month of June 2012 with our SID monitor. During this month we have detected 24 events. We believe that this number of events is sufficient to select a good method among those proposed for SIDs classification. Indeed, longer periods of VLF recording should be more rigorous.

3.1 Measure of SIDs durations from raw VLF data

We take directly from the raw data the chronology of the event, *i.e.*, the starting time, the time corresponding to the maximum and the end of the SID event using the methodology indicated by the AAVSO's report (AAVSO 2015) and as indicated by the methodology document SWPC (SWPC/NOAA 2015). This method is effective only near solar noon because during this period the VLF record is relatively flat and stable, being distant from the sunrise and sunset part of VLF data.

As we can see in Fig. 3, it is difficult to accurately collect these data for the first and the third SID. In fact, the first SID is almost completely hidden

by the background noise while the third one performs its decay near the period of the sunset. These two peaks require more data processing in order to provide accurate values for their chronology.

3.2 Subtraction method: quiet day-active day

The first step in the signal processing is to eliminate the diurnal variation of the signal obtained without any SID. We chose a signal recorded in a day preferably with little noise and should be the nearest one to the active day of interest (which have signatures of SIDs) in order to keep identical conditions and better isolate the direct effects of solar flares. This day can be referred as a reference day (or control day). As we mentioned before, we only focus on the stable diurnal period, the time interval between sunset and sunrise. So we apply a cubic spline interpolation (the yellow line in Fig. 5) to this part of signal. This later will be used as a baseline that we will subtract from each active day (a day with SIDs, red line in Fig. 5). This method allows us to better isolate SIDs events and reduces the noise for a better detection of weak SIDs (*e.g.*, after applying this method the SID induced by solar flare C3.5 will be much clearer).

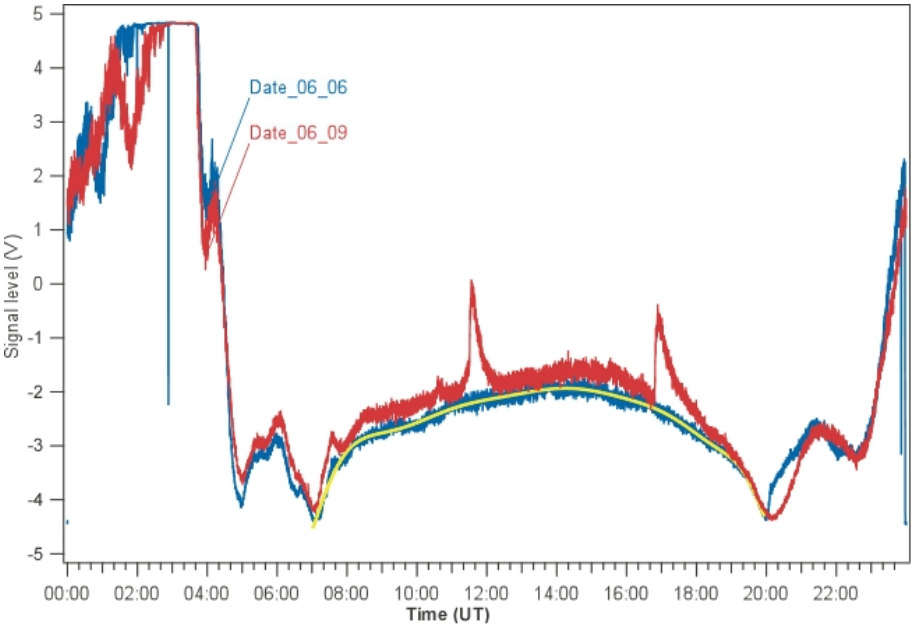

Fig. 5. Visualization of the two recording dates of 6 June 2012 (blue) and 9 June 2012 (red). The yellow line corresponds to a cubic spline of the selected reference day 6 June 2012, between the time 07:00 and 20:00 UT.

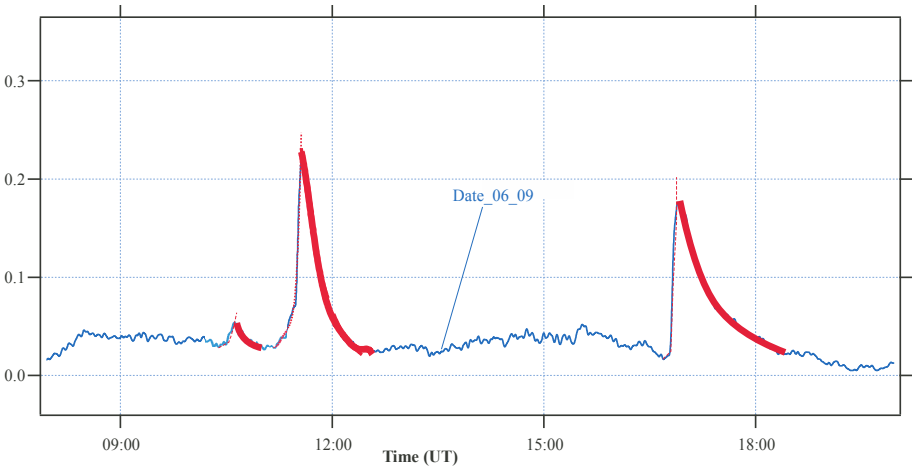

Fig. 6. Signal obtained after subtracting the cubic spline fit of 6 June 2012 from the record of the 9 June 2012 for the period between 07:00 and 20:00 UT data.

In Fig. 6, after applying this subtraction method, we find that AAVSO's methodology to classify SIDs is much easier than before and appreciably improves our estimates. Also, the small peak at 10:32 UT is much clearer and allowing the better determination of its duration.

3.3 Method of exponential decay

This method is combined with the subtraction method described in the previous section. As we have already mentioned in Section 2, the shape of recorded SIDs in present work shows two parts, an increase followed by a decrease in amplitude. The first part, which is very brief, corresponds approximately to the ionization phase of the ionosphere by X-ray radiations and the second part, with longer duration, corresponds approximately to the phase of recombination of the ionosphere and characterized by an exponential decay. The limit between these two parts is not always precisely defined because the time when ionization phase passes in recombination phases is not exactly amplitude independent. Also, the amplitude is not necessarily a monotonic function of the electron density and we cannot generally say that the time when amplitude finishes its increase is the same as the time of electron density maximum (Nina *et al.* 2012). We focus here our attention on the second part of the signal and we propose a reliable method for the determination of the recombination time for each detected SID.

The instant selected for characterizing the end time is taken as the exponential decay rate (Fig. 6, red line). This solution avoids the difficulty we encounter when the recovery time is very long and no end time is clearly dis-

tinguishable. Measurements of the duration of the SIDs by this method show a remarkable reduction of the duration (about half) in comparison with AAVSO's methods.

3.4 Empirical Mode Decomposition method

There are many methods of data processing (Fourier, wavelets), which are based on the decomposition of signals formed on the basis of the Eigen modes. The Empirical Mode Decomposition (EMD) is a data analysis method developed by Huang (Huang *et al.* 1998) for the study of oceanographic data. Subsequently, it has been introduced in other areas. The main objective of the EMD is to define decompositions that do not depend on the choice of a particular base. In addition, the EMD method is particularly well suited for the study of non-stationary signals, as is the case for our signals. In contrary, this method is not well suited for events that encompass several perturbations, as it is sometimes the case here.

We use the EMD software, a C compiled program, developed by Loudet (2009). The graphical user interface developed in our application (SIDLab) calls this program out and this greatly facilitates the comparison between various combinations of Intrinsic Mode Functions (IMF) and the GOES data.

Figure 7 shows again the three SIDs of 9 June 2012, analyzed with EMD method. We have selected the fifth mode (IMF5) to assess the duration of the three SIDs resulting from solar flares C1.6, M1.8, and M1.9, respective-

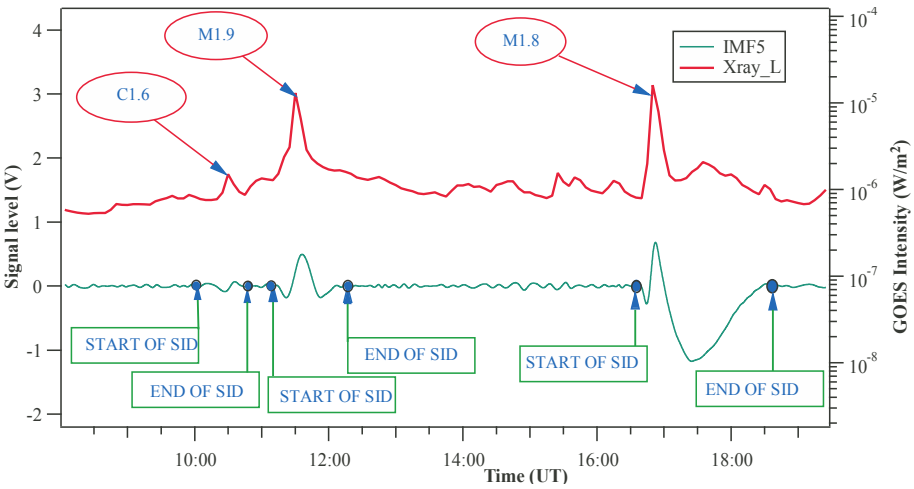

Fig. 7. Plot of GOES spectrum with the IMF5 component of the VLF data. The SIDs are interpreted by a strong oscillation around the zero of the data amplitude. The return to zero fixes the end of each SID event.

ly. By observing carefully Fig. 7, we can notice the improvement obtained by the EMD analysis regarding the temporal analysis of the events. Return to zero in the IMF component is more obvious to detect than the return to a level corresponding to normal conditions of propagation in the raw data. In contrary the determination of the exact position of the starting point of the SID is not always obvious. So basing on some additional criteria, *e.g.*, that the start of the SID must come after the start of the flare, and also taking into account the change in tendency which must be significant, we can better fix this position.

3.5 Noise reduction of the VLF signals

In order to reduce the noise we got after the subtract method (Fig. 6), we applied a noise reduction to the VLF raw data based on the EMD technique. Again, a special function is built in our application to easily achieve this operation. In this case, it eliminates the first three IMF (Loudet 2009) from raw VLF signal, getting a clearer, signal such as the signal in Fig. 8 (green line).

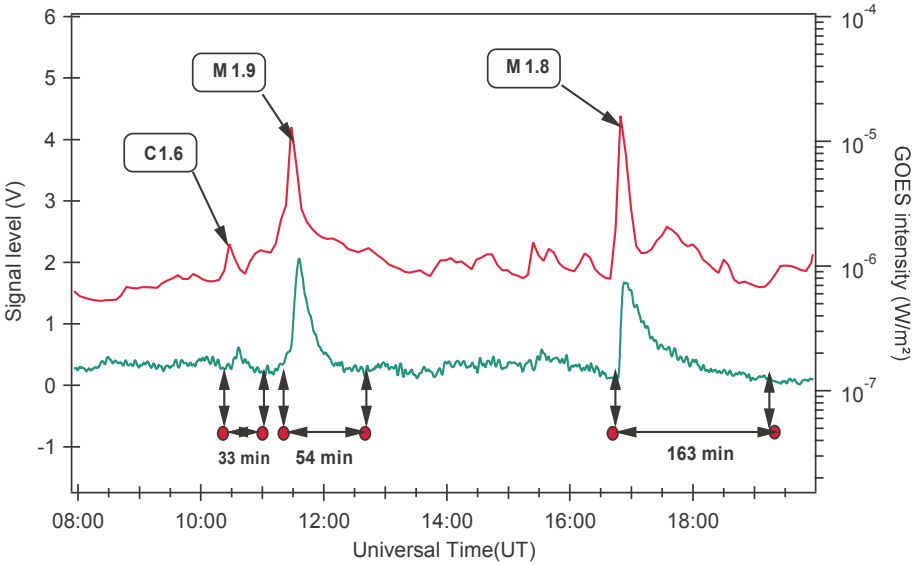

Fig. 8. Correlation between VLF recording (green) with that of GOES15 satellite (red), for the day 9 June 2012. The classification is indicated on the curves.

4. DISCUSSION

In Table 1, we assigned to each event occurred during June 2012 the durations measured by the different methods. We referred to each of these methods as follows: τ_{M1} for duration measured from the raw signal, τ_{M2} for the

subtraction method, τ_{M3} for the exponential decay, τ_{M4} for the EMD method, and τ_{M5} for the noise reduction method.

Table 1

Estimated durations for each method

Date	Number of SID	M1[a)]	M2[b)]	M3[c)]	M4[d)]	M5[e)]	GOES[f)]	GOES class[g)]
7 June 2012	1	38	60	38	–	65	18	C2.7
7 June 2012	2	98	117	65	42	42	26	C9.1
9 June 2012	3	54	89	45	47	58	15	M1.9
9 June 2012	4	43	97	43	41	69	11	M1.8
13 June 2012	5	39	108	34	16	44	5	C1.3
13 June 2012	6	153	404	95	71	82	122	M1.2
13 June 2012	7	31	49	42	48	57	10	C2.7
14 June 2012	8	41	61	39	27	45	17	C5.0
14 June 2012	9	166	328	75	97	71	124	M1.9
15 June 2012	10	62	146	40	65	50	26	C3.4
15 June 2012	11	–	82	55	–	35	22	C2.0
16 June 2012	12	66	87	60	52	73	15	C1.8
17 June 2012	13	53	109	36	42	28	10	C3.9
20 June 2012	14	51	119	44	47	77	23	C3.1
27 June 2012	15	34	38	22	28	31	7	C3.4
28 June 2012	16	56	63	31	39	53	8	M2.4
29 June 2012	17	74	79	29	38	43	5	C2.9
30 June 2012	18	80	73	37	–	44	9	M2.2
30 June 2012	19	48	44	34	34	47	15	C4.4
30 June 2012	20	58	69	37	39	45	54	C2.7
30 June 2012	21	54	49	25	27	52	6	M1.0
30 June 2012	22	37	91	47	92	70	8	M1.6

Explanations: all the values are in minutes; (a) raw VLF signal, (b) raw minus reference, (c) exponential decay method, (d) EMD, (e) noise reduction method, (f) GOES duration, and (g) solar flare class associated with each SID.

The question that comes out from all these measurements is: which of these methods is the most relevant to classify SIDs according to their duration? Part of the answer can be formulated by the question: which are the best criteria we have to define in order to give a reliable classification. In our opinion, reliable classification should satisfy the following two criteria:

(i) Which method gives the best correlation to GOES classification?

(ii) Which method reveals less dispersion?

These two criteria act in the same direction, which consist to circumvent the overall terrestrial conditions (climate, ionospheric variability, noises, *etc*.). To fulfil these two criteria, we define two variables:

(i) Variable x_{Gi} measuring the discard between the duration of the proposed methods τ_{Mi} with the duration obtained by GOES Flux τ_G:

$$x_{Gi} = \tau_G - \tau_{Mi} \tag{1}$$

(ii) Variable x_{Mi} measuring the discard between the averages of the methods $\tau_{\overline{Mi}}$ (without GOES) with each method described in Section 4:

$$x_{Mi} = \tau_{Mi} - \tau_{\overline{Mi}} \tag{2}$$

Individual Standardized Deviation that takes into account the dependency of the error on the size of flare is defined for each proposed method. This parameter, named G_{Mi} and defined below, binds the two criteria in a unique quantity:

$$G_{Mi} = \frac{\left| x_{Gi} * x_{Mi} \right|}{d^2} \tag{3}$$

where $d = \tau_G - \tau_{\overline{Mi}}$ is a normalization factor. We analyse the duration of all the SIDs (21 events) measured during one month by means of the Principal Component Analysis (PCA). The aim of this technique is to reduce a large number of variables to a much smaller number of Principal Components (PCs) that best describe the data in terms of the variance. These PCs are a linear combination of the physical set of variables (SIDs events). This approach enables effective visualization, regression and classification of the multivariate data (Brereton 1992). In our case, it will help us to easily show the correlation that may exist between the different methods by clustering them. In our study, the binding parameters G_{Mi} are considered as the individual and the SID events as the variables. In this way we built a matrix of dimension 5*21 parameters, say GM_{ij}, where $i = 1 \ldots 5$ corresponds to the columns of Table 1 and $j = 1 \ldots 21$ to the lines. This statistical analysis is done using 'R' software (https://www.r-project.org/).

As shown in Fig. 9, the first two principal components (Dim1 + Dim2) explain 86.98% of the variance in the data matrix and the first one (Dim1) alone explains more than 73% of the variance. According to Cattell's scree test, the first two components are sufficient to get the maximum dispersion of the data. We can clearly see here that M_{G4}, M_{G5}, and M_{G3} are close both to each other and to the centre (0, 0) of the diagram relative to the M_{G1} and M_{G2}, which are more dispersed and farther from the centre. We recall here that we use the AAVSO method to define the duration of the SID in M_{G1}.

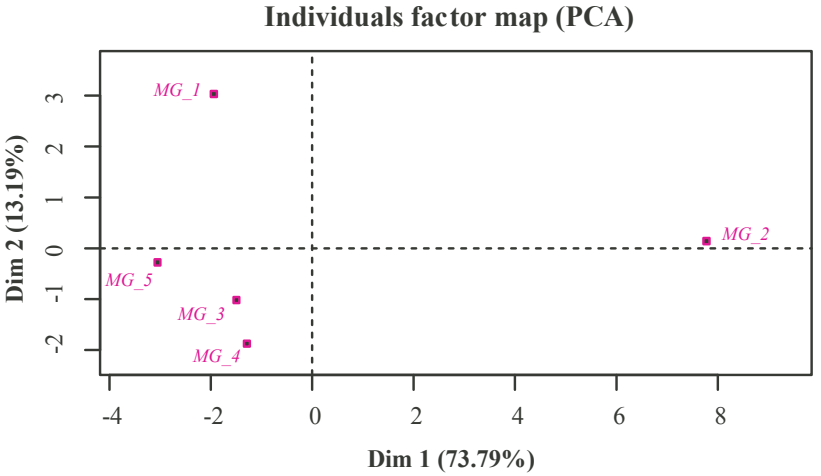

Fig. 9. Scores plots of the methods from PCA: first plane (Dim1, Dim2) with cumulative percentage of variance of 86.98%.

Those results indicate that the M_{G4}, M_{G5}, and M_{G3} methods based on EMD technique, noise reduction and exponential decay, respectively, are closer to the GOES duration and less dispersed than the last two methods based on direct measure of the duration. In other words, this means that these three methods better satisfy the two criteria. Furthermore, the parameter M_{G3} which is the closest to the centre (0, 0) of the diagram indicates that it is least dispersed among the three and thus the exponential decay is the most recommended method to determine the duration of the SID and accordingly its classification.

In the light of those results, we can assume that classification based on the exponential decay method will better correlate the GOES classification. To confirm this point, we use the Spearman's rank correlation (Gibbons and Chakraborti 2011) which seeks correlations between non-parametric data as our own. The results of the test are listed in Table 2.

Table 2

Non-parametric Spearman correlation rank

Method	*p* value	Rho
M3	6.0410^{-5}	0.741
M4	0.0043	0.593
M2	0.0121	0.483
M1	0.0281	0.425
M5	0.0503	0.359

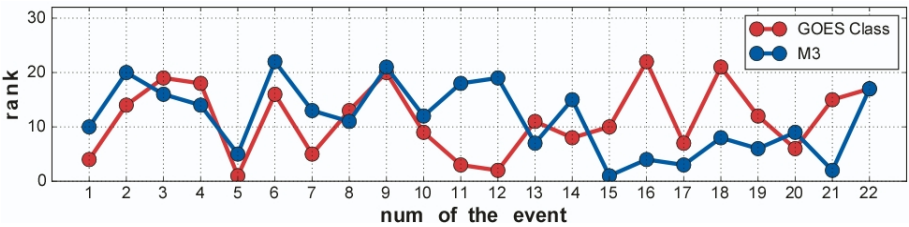

Fig. 10. Ranking of the SIDs based on their duration (in blue) and the ranking of the flares based on GOES intensity (in red).

We note the first rank of the method 3 with the smallest p value indicating a "strong evidence against null hypothesis" attesting a very significant test and a correlation coefficient "Rho" of around 0,74 which indicate a "strong" correlation according to the hierarchy established by the Spearman statistics. We give in Fig. 10 the SIDs ranking based on their duration together with the flares ranking based on their GOES intensities. For example, for the first event (7 June 2012) the GOES flare is at the 4th rank (last column in Table 1) whereas the M3 method places it at the 10th rank. We can notice the good correlation between these two line graphs based on their similar behaviour. The same comparisons are done with the other methods but none of them showed such a good agreement with the GOES ranking which is in accordance with the values of Table 2.

5. CONCLUSION

The main goal of this work is to define objective criteria that allow us to create a stable and reliable classification of the SID on the basis of their duration. We investigate for this purpose different methods that minimize the dispersion of the values independently of the activity and noise present on the VLF recording. The exponential decay method (M3) seems to give a satisfactory result for the classification, showing a strong correlation with the satellite intensity classification. Moreover, this method is well adapted to analyze a weak signal (like the C1.6 present in our VLF recording). We plan to experiment with all these methods using a greater amount of VLF and LF recording and with all different shapes of SIDs described in Section 2 in order to improve and confirm this result. Future developments of the "SIDLab" application will help us to get this goal.

Acknowledgments. To the support and the encouragements of Prof. Deborah Scherer from Stanford University, USA. The authors also thank STO (Société Tunisienne d'Optique) and ICTP through the Affiliated Center, which supported this work.

References

AAVSO (2015), Reducing data gathered by VLF monitoring systems, American Association of Variable Star Observers, Cambridge, MA, USA, available from: https://www.aavso.org/sid-reducing-data (accessed: 11 June 2015).

Brereton, R.G. (ed.) (1992), *Multivariate Pattern Recognition in Chemometrics: Illustrated by Case Studies*, Elsevier, Amsterdam.

Correia, E., P. Kaufmann, J.-P. Raulin, F. Bertoni, and H.R. Gavilán (2011), Analysis of daytime ionosphere behavior between 2004 and 2008 in Antarctica, *J. Atmos. Sol.-Terr. Phys.* **73**, 16, 2272-2278, DOI: 10.1016/j.jastp.2011.06.008.

Dahlgren, H., T. Sundberg, A.B. Collier, E. Koen, and S. Meyer (2011), Solar flares detected by the new narrowband VLF receiver at SANAE IV, *S. Afr. J. Sci*. **107**, 9/10, 40-47, DOI: 10.4102/sajs.v107i9/10.491.

Dellinger, J.H. (1937), Sudden disturbances of the ionosphere, *Proc. Inst. Radio Eng.* **25**, 10, 1253-1290, DOI: 10.1109/JRPROC.1937.228657.

Gibbons, J.D., and S. Chakraborti (2011), *Nonparametric Statistical Inference*, Springer, Berlin Heidelberg, DOI: 10.1007/978-3-642-04898-2_420.

Grubor, D.P., D.M. Šulić, and V. Žigman (2008), Classification of X-ray solar flares regarding their effects on the lower ionosphere electron density profile, *Ann. Geophys*. **26**, 7, 1731-1740, DOI: 10.5194/angeo-26-1731-2008.

Huang, N.E., Z. Shen, S.R. Long, M.C. Wu, H.H. Shih, Q. Zheng, N.C. Yen, C.C. Tung, and H.H. Liu (1998), The empirical mode decomposition and the Hilbert spectrum for nonlinear and non-stationary time series analysis, *Proc. Roy. Soc. A* **454**, 1971, 903-995, DOI: 10.1098/rspa.1998.0193

Loudet, L. (2009), Application of Empirical Mode Decomposition to the detection of Sudden Ionospheric Disturbances by monitoring the signal of a distant Very Low Frequency transmitter, available from: http://sidstation.loudet.org/emd-en.xhtml (accessed: 11 June 2015).

Mitra, A.P. (1975), D-region in disturbed conditions, including flares and energetic particles, *J. Atmos. Terr. Phys*. **37**, 6, 895-913, DOI: 10.1016/0021-9169(75)90005-7.

Nina, A., V. Čadež, V. Srećković, and D. Šulić (2012), Altitude distribution of electron concentration in ionospheric D-region in presence of time-varying solar radiation flux, *Nucl. Instrum. Meth. Phys. Res. B* **279**, 110-113, DOI: 10.1016/j.nimb.2011.10.019.

Rosen, R.D., and D.L. Johnson (2004), Service assessment. Intense space weather storms October 19 – November 07, 2003, U.S. Department of Commerce, National Oceanic and Atmospheric Administration, National Weather Service, Silver Spring, MD, USA, available from: http://www.nws.noaa.gov/os/assessments/pdfs/SWstorms_assessment.pdf (accessed: 30 September 2015).

Scherrer, D., M. Cohen, T. Hoeksema, U. Inan, R. Mitchell and P. Scherrer (2008), Distributing space weather monitoring instruments and educational materials worldwide for IHY 2007: The AWESOME and SID project, *Adv. Space Res.* **42**, 11, 1777-1785, DOI: 10.1016/j.asr.2007.12.013.

SWPC/NOAA (2015), GOES X-ray Flux, Space Weather Prediction Center, National Oceanic and Atmospheric Administration, Boulder, USA, available from: http://www.swpc.noaa.gov/products/goes-x-ray-flux (accessed: 11 June 2015).

Thomson, N.R., and M.A. Clilverd (2001), Solar flare induced ionospheric D-region enhancements from VLF amplitude observations, *J. Atmos. Sol.-Terr. Phys.* **63**, 16, 1729-1737, DOI: 10.1016/S1364-6826(01)00048-7.

Thomson, N.R., C.J. Rodger, and M.A. Clilverd (2005), Large solar flares and their ionospheric D region enhancements, *J. Geophys. Res*. **110**, A6, DOI: 10.1029/2005JA011008.

Received 3 April 2016
Received in revised form 13 August 2016
Accepted 18 October 2016